Isolators, Polarizers, and Other Optical Waveguide Devices Using a Resonant-Layer Effect

Jacob M. Hammer, *Life Fellow, IEEE, Member, OSA*, Gary A. Evans, *Fellow, IEEE, Member, OSA*, Gokhan Ozgur, *Student Member, IEEE*, and Jerome K. Butler, *Fellow, IEEE*

***Abstract*—This paper investigates the effect of a high-refractive-index layer added onto the clad layer of an optical waveguide. With proper design, the value of the fundamental mode's confinement factor in the added layer can exhibit a resonance. This resonance depends on the added layer's location, thickness, complex index, and wavelength of operation. If loss is incorporated into this added layer, relatively small changes in waveguide properties can result in large changes in loss. This phenomenon is referred to in this paper as the resonant-layer effect (RLE). A number of devices, including isolators, polarizers, and modulators, can be made and/or improved by using the RLE. As examples, this paper describes an integratable isolator giving 240-dB/cm isolation and 13-dB/cm insertion loss, an integratable polarizer with 90-dB/cm rejection and about 0.8-dB/cm insertion loss, and a 300-μm-long modulator requiring electric fields of ± 5 V/μm for $\sim 45\%$ intensity modulation. In general, the resonant layer need not be epitaxial with the waveguide, allowing for integration with a variety of material systems.**

***Index Terms*—Integrated optics, magnetooptic Kerr effect, modulation, optical isolators, optical polarizers.**

I. Introduction

A SECOND peak of the fundamental mode can appear in a high-refractive-index layer added onto or within the clad of an optical waveguide. The overall waveguide loss can be dominated by the loss in the added layer and used to selectively suppress guided modes. This effect may be used to enhance the operation of a number of optical waveguide devices. The appearance of the secondary field peak in conjunction with the suppression of secondary guided modes is sensitive to the location, refractive index, loss, and thickness of the added layer and to the wavelength of operation. This phenomenon is called the *resonant-layer effect* (RLE).

A number of devices, including isolators, polarizers, modulators, grating-feedback reflectors, and grating outcouplers can be made and/or improved by using the RLE. The appearance of RLE generally results in relatively high modal loss. Since the RLE is sensitive to the physical characteristics of the waveguide, relatively small changes in waveguide properties can result in large changes in loss. This RLE concept is easily integrated into any optical waveguide.

The RLE is similar to a resonance effect observed in channeled-substrate-planar (CSP) lasers that accidentally had a nonuniform Al composition in the channel [1].

Many useful devices rely on changes in modal loss. Isolators result from loss changes with propagation direction. Amplitude modulators result from loss changes in response to a physical input such as an electric or magnetic field. A space-periodic change in loss results in a diffraction grating. In polarizers, the loss changes with polarization.

For example, a transverse electric (TE) mode may show a strong RLE and thus have a large secondary peak in the resonant layer (RL), while a transverse magnetic (TM) mode of the same structure will have no secondary peak in the RL, giving rise to a polarization-sensitive filter. A number of examples of how RLE gives rise to useful devices are given hereafter.

Briefly, to obtain the RLE, a relatively high-index layer (usually containing loss) is deposited on or within the clad layer of an optical waveguide, which is referred to here as the RL, or *resonant layer*. The real part of the refractive index of the RL must be higher than that of the clad. In this case, at the correct thickness, and for the correct range of the complex index of the RL, a secondary peak of the modal field will exist in the RL. This means that a substantial fraction, in some cases $\approx 25\%$, of the guided-mode intensity is confined to the RL. Under these conditions, small changes in the propagation constant of the guided mode will result in large changes in the confinement factor of the RL. The waveguide modal propagation constant may be changed in several ways.

1) There can be a polarization change. This leads to a polarizer.
2) There can be a change in propagation direction in conjunction with an RL made from ferromagnetic materials, which, in the presence of a magnetic field, show magnetooptic effects (Faraday/Kerr effect). This leads to an isolator that may be integrated with a wide variety of material systems. As a corollary, varying an applied magnetic field can result in modulation.
3) There can be a change in applied electric fields in conjunction with an RL or other layers that exhibit electrooptic effects such as the Pöckel's effect. This leads to intensity modulation.
4) There can be a change in the wavelength. Here, the loss layer acts as a wavelength filter.
5) Finally, there can be a periodic spatial variation of the thickness (or complex index) of the RL itself. In this case,

Manuscript received October 3, 2003; revised January 29, 2004. This work was supported in part by the Texas Higher Education Coordinating Board under Grants TDT 003613-0019-2001 and ATP 003613-0038-2001, the U.S. Army Space and Missile Defense under SBIR Contract DASG60-02-P-0099, and Photodigm, Inc., Richardson, TX.

J. M. Hammer is with Photonics Consulting, Annapolis, MD 21401 USA (e-mail: jakehammer@ieee.org).

G. A. Evans, G. Ozgur, and J. K. Butler are with the Electrical Engineering Department, Southern Methodist University, Dallas, TX 75275-0338 USA (e-mail: gae@engr.smu.edu).

Digital Object Identifier 10.1109/JLT.2004.831088

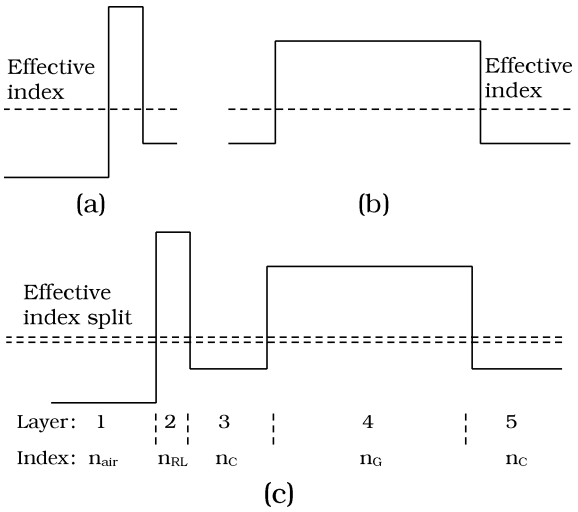

Fig. 1. Geometry of the basic RLE architecture. (a) Index profile of the left subwaveguide with its modal effective index n_A, (b) the index profile of the right subwaveguide with its modal effective index n_B, and (c) the refractive-index profile and the effective indexes of the waveguide modes.

the amplitude of the resulting grating can be greatly magnified. A grating period chosen to outcouple radiation can increase the loss of the RL. An RL also allows flexibility in the placement of gratings in waveguides.

Phase-matched waveguides cited in the literature are commonplace. Directional couplers/modulators are examples [2]. Despite this, to the authors' best knowledge, the exploitation of the secondary field peak in one "subwaveguide" when the other "subwaveguide" is excited [3] has not been exploited in the manner described in this paper. Specifically, if sufficient loss is added to the RL, the secondary peak has significant amplitude over a limited thickness and index range, in contrast to the loss-free case in which the amplitude of the secondary peak may increase monotonically with RL thickness until the RL becomes the principle guide.

II. Theory and Method of Finding the Required Thickness of the RL to Observe the RLE

The appearance of a secondary peak may be understood by considering the fields of the two separate three-layer waveguides in Fig. 1(a) and (b), and the field of the composite five-layer waveguide in Fig. 1(c). If the two waveguides are in close proximity [Fig. 1(c)], they become subwaveguides of the composite waveguide. Although the fundamental mode of the composite waveguide will have energy distributed in both subwaveguides, if the waveguides are dissimilar, then typically, there is little energy in the secondary waveguide and most of the energy in the primary waveguide. Conversely, if the subwaveguides are identical, the energy is equally distributed between them.

By considering the transverse wave vectors that correspond to each subwaveguide, we can understand how to obtain a significant secondary peak in one of the subwaveguides. If the thickness and index of the secondary waveguide [layer 2 in Fig. 1(c)] is appropriately chosen, maximum energy is transferred between the two subwaveguides. Layer 2 can be crudely viewed as an "antireflective" coating that allows the traveling

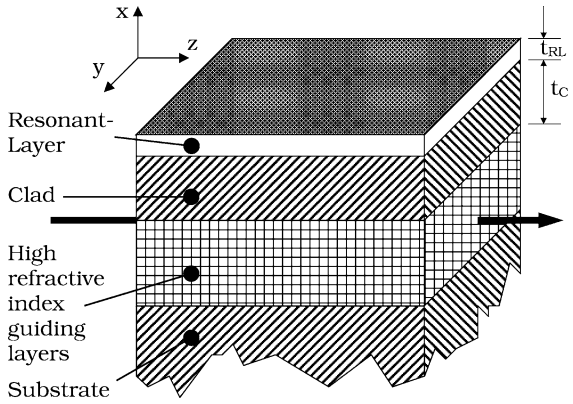

Fig. 2. Schematic of a generic RLE optical waveguide structure.

waves corresponding to the transverse wave vectors in layer 4 to penetrate into both layers 2 and 1, thereby maximizing the secondary field peak. Of course, the exact thickness and index value of layer 2 depends on the thicknesses and indexes of all five layers.

Based on this physical model, the correct thickness range of the RL may be found by the following method (note that to obtain the secondary peak, the real part of the complex refractive index of the RL must be greater than that of the cladding layer on which the RL is deposited, and lowest order planar waveguide modes are assumed). First, take the primary waveguide to be a three-layer planar waveguide consisting of an infinitely thick substrate and a cover layer with a refractive index equal to that of the clad n_C and a guide layer with index n_G and thickness t_G equal to those of the device under study. Find the effective index (N_G) of the lowest order mode of this waveguide. Then, consider the secondary waveguide to be an asymmetric-three-layer-planar guide [Fig. 1(a)] consisting of a substrate made of the same material as the clad layer of the device, a high-index layer with refractive index equal to the real part of the RL layer n_{RL}, and air or vacuum as the upper layer. Calculate the effective index for this planar waveguide (N_{RL}) as a function of the RL thickness t_{RL}. The value of t_{RL} at which $N_{\mathrm{RL}} = N_G$ will be close to the optimum required for the RLE. If no match is found, then RLE will not be obtained. In this case, the thickness or other parameters of the principal guide may be varied to achieve the desired match. A similar calculation can be done for cases in which the RL is covered with a low-index layer other than air. This would be the case if the RL were "buried" in cover material.

A second method to estimate the thickness range of the RL is to calculate the cutoff thickness h of the lowest order mode for the asymmetric planar waveguide [Fig. 1(a)] and consider thicknesses where $h < t_{\mathrm{RL}} < 2h$ and where h is found from the formula [4]

$$h = \left[\frac{\left(\frac{\lambda}{2\pi}\right)}{(n_{\mathrm{RL}}^2 - n_C^2)^{1/2}}\right] \tan^{-1}(a^{1/2}). \tag{1}$$

a is given by

$$a = a_{(\mathrm{TE})} = \frac{(n_C^2 - 1)}{(n_{\mathrm{RL}}^2 - n_C^2)} \tag{2}$$

TABLE I
WAVEGUIDE LAYERS FOR A POLARIZER

Center Wavelength λ = 1.55 μm			
Material	Loss, α (cm^{-1})	Refractive Index	Thickness (μm)
Air	0.0	1.0	-
Resonant Layer Polymer with dye	4.0×10^2	1.54	TE t_{RL} = 0.63, h = 0.619 TM t_{RL} = 0.76, h = 0.714
Quartz (p-) clad	0.0	1.447	t_C = 4.0
Doped quartz core	0.0	1.452	10.0
Quartz Substrate	0.0	1.447	-

Waveguide layers for a polarizer using a simple quartz-based waveguide with a BP Polymer RL [6] containing an absorbing dye. The cutoff thickness $h = 0.619$ (TE) and $h = 0.714$ (TM), giving a ratio of $t_{\rm RL}/h = 1.02$ (TE), 1.06 (TM).

for TE modes, and

$$a = a_{(\rm TM)} = a_{(\rm TE)} n_F^4. \tag{3}$$

for TM modes.

$n_{\rm RL}$ is the real part of the refractive index of the RL, which is considered to be the guiding layer for the purpose of this cutoff calculation. n_C is the refractive index of the clad layer, which is considered to be the substrate for the purpose of this cutoff calculation. n_F is the ratio of $n_{\rm RL}$ to the refractive index of the lowest index clad layer (air, in this case).

Generally, the optimum thickness can be further refined by calculating the maximum confinement factor ($\Gamma_{\rm RL}$) of the RL layer as a function of the RL thickness for the wavelength and polarization mode considered. This may be done using well-known analytic means or software such as MODEIG/WAVEGIDE [5].[1] The $t_{\rm RL}$ value at which $\Gamma_{\rm RL}$ is maximized is close to the optimum thickness for the device in question. In doing this calculation, one usually avoids solutions where the RL becomes the dominant guiding layer.

The thickness of the clad, t_C influences the value of $\Gamma_{\rm RL}$ and has a secondary influence on the optimum thickness of the RL. In many cases, t_C is chosen so that $\Gamma_{\rm RL}$ is less than about 0.25, which implies that less than 25% of the field intensity is confined to the RL. Finally, the loss of the RL is chosen to maximize modal loss while still maintaining the fundamental mode of the complete waveguide. The peak-resonant wavelength may be tuned by changing the thickness of the RL.

III. RLE POLARIZERS

Consider the waveguide structure illustrated in Fig. 2. A high-index layer with loss is applied on top of the clad layer of a waveguide consisting of undoped and doped quartz layers (similar to layers used in optical fibers). In this example, the RLE will result in a polarizer and broad-band wavelength filter. Each layer of this waveguide is listed in Table I. The RL is a polymer, such as perfluorocyclobutyl polymer plastic BP [6], containing a dye that has modest absorption in the 1.55-μm wavelength region and is placed as the RL of the waveguide shown in Fig. 2. Near-field intensities illustrating the secondary peak for the lowest order TE and TM modes are plotted in Fig. 3(a) and (b) at a wavelength of 1.55 μm and an RL loss of $\alpha_{\rm RL} = 400\ \ {\rm cm}^{-1}$. In Fig. 3(a), at an RL thickness $t_{\rm RL} = 0.76\ \mu$m a strong secondary peak in the loss layer

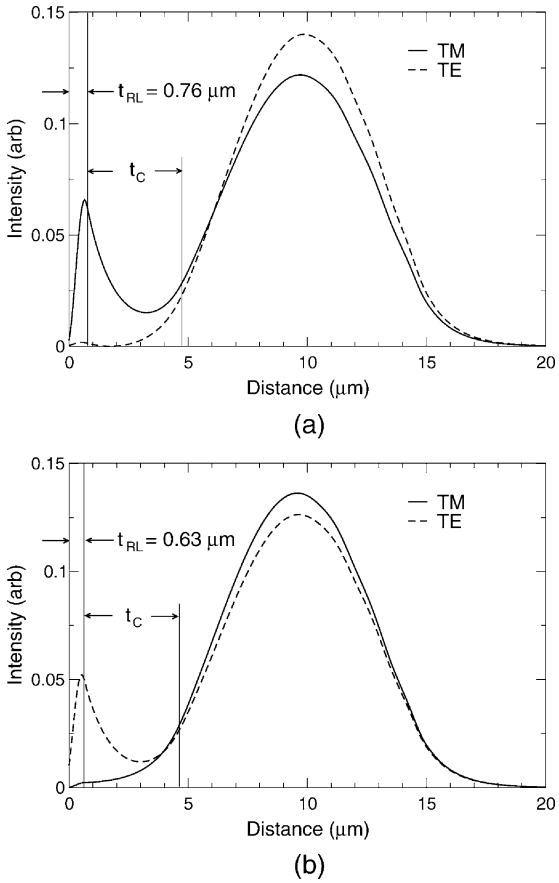

Fig. 3. Near-field intensity for quartz waveguide with a doped BP polymer RL showing RLE. RL thickness: (a) $t_{\rm RL} = 0.76\ \mu$m, and (b) $t_{\rm RL} = 0.63\ \mu$m. Wavelength of operation is $\lambda = 1.55\ \mu$m.

[1]A revised version of the software described in [5] is available at http://engr.smu.edu/ee/smuphotonics/Modeig.htm

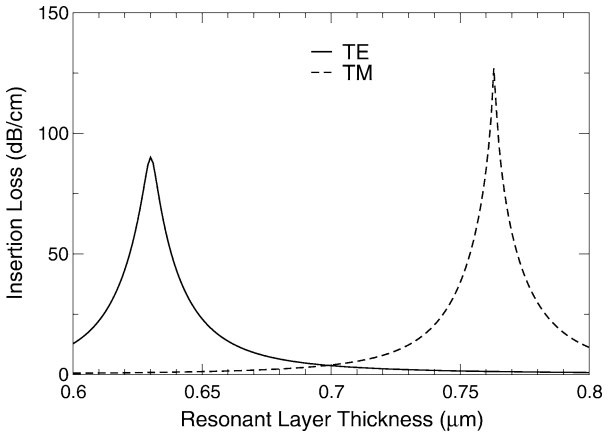

Fig. 4. Insertion loss as a function of the RL thickness for a quartz waveguide with a doped BP Polymer RL. The solid line is the TE_0 mode, and the dashed line is the TM_0 mode. RL loss is $\alpha_{\mathrm{RL}} \approx 220\ \mathrm{cm}^{-1}$. Wavelength of operation is $\lambda = 1.55\ \mu$m.

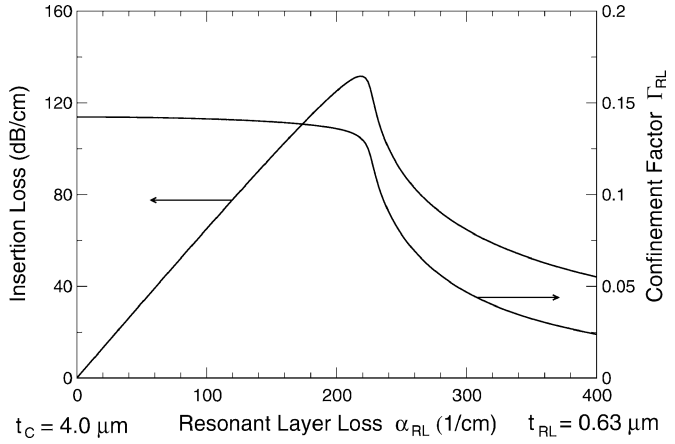

Fig. 5. Insertion loss and BP polymer RL confinement factor of the TE mode at $\lambda = 1.55\ \mu$m as function of a doped BP polymer RL loss for a quartz waveguide (Table I and Fig. 2). The RL thickness t_{RL} is chosen to give a TM polarizer. The TM insertion loss is below 3 dB/cm over the range plotted. RL loss is $\alpha_{\mathrm{RL}} \approx 220\ \mathrm{cm}^{-1}$.

occurs for the TM mode, and there is no peak for the TE mode. Here, maximum absorption of the lowest order TM mode takes place. In Fig. 3(b) where $t_{\mathrm{RL}} = 0.63\ \mu$m, the secondary peak occurs for the TE mode, which will result in maximum absorption of this mode. In both figures, the thickness of the cladding layer t_C is 4.0 μm.

The effect of these secondary peaks on the modal transmission is illustrated in Fig. 4, which shows the insertion loss as a function of the RL thickness. The solid line is for the TE_0 mode. The dashed line is for the TM_0 mode. At $t_{\mathrm{RL}} = 0.63\ \mu$m, the TE shows maximum absorption, while at $t_{\mathrm{RL}} = 0.76\ \mu$m, the TM mode shows maximum absorption. The absorption passes through a maximum as the thickness of the RL is increased. This reflects the magnitude of the secondary peak that also passes through a maximum as the thickness is varied. For each polarization mode, t_{RL} is slightly larger than the cutoff thickness (h) of the center layer of the secondary three-layer waveguide calculated as described in Section II.

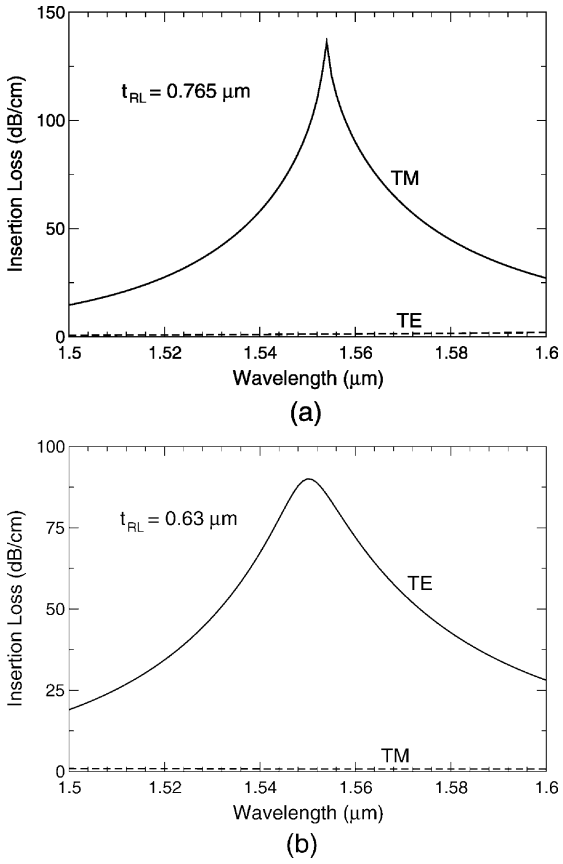

Fig. 6. Band-stop characteristic for quartz waveguide with doped BP polymer RL showing RLE. RL loss is $\alpha_{\mathrm{RL}} = 220\ \mathrm{cm}^{-1}$. (a) $t_{\mathrm{RL}} = 0.765\ \mu$m. (b) $t_{\mathrm{RL}} = 0.63\ \mu$m.

There is a limited range of RL absorption values over which such "resonant" secondary peaks may be observed, and a maximum value of modal (insertion) loss, which is illustrated in Fig. 5. Fig. 5 shows both the insertion loss and confinement factor of the TE mode at $\lambda = 1.55\ \mu$m as a function of layer loss. In this case, the maximum RLE giving rise to the highest insertion loss occurs at an RL loss $\alpha_{\mathrm{RL}} \approx 220\ \mathrm{cm}^{-1}$. At this peak value of insertion loss, the confinement factor is still very close to its maximum value that occurs at zero layer loss. In this plot, the RL thickness t_{RL} is chosen to give strong TE absorption. The TM insertion loss is below 3 dB/cm over the loss range plotted, as suggested by Fig. 4. Similar behavior is observed if the thickness is chosen to give strong TM absorption. In general, there is an optimum value of RL loss, which maximizes the modal (or insertion) loss for each particular device.

Fig. 6(a) is a plot of the insertion loss for both the TE_0 and TM_0 modes as a function of wavelength for $t_{\mathrm{RL}} = 0.76\ \mu$m and an RL loss of 220 cm^{-1}. The strong absorption of the TM mode (≈ 140 dB/cm) and the weak absorption of the TE mode (≈ 1 dB/cm) is the behavior of a TE polarizer. Fig. 6(b) is a similar plot for $t_{\mathrm{RL}} = 0.63\ \mu$m. This case illustrates a good and rather broad-band TM polarizer with 90-dB/cm absorption of the TE mode and a very weak absorption of the TM mode (0.82 dB/cm). Thus, the RLE can be used to make an efficient polarizer and wavelength filter. The thickness of the clad t_C is chosen according to the discussion in Section II.

IV. Isolators Using the RLE

An isolator may be obtained if the RL in Fig. 2 is made from a ferromagnetic material. Isolators with useful isolation and low forward insertion loss are produced when the RLE is present. As explained in detail hereafter, the same arrangement acts as an isolator absent the RLE, but with much higher forward insertion loss, resulting in poor performance [7].

A biasing magnetic field ($H(\pm)$) applied in the lateral (y) direction results in a nonreciprocal change of the complex propagation constant of a TM-like guided mode due to the magnetooptic Kerr effect [7]–[9]. Thus, the loss for guided light traveling in the $+z$ direction is different than the loss in the $-z$ direction, resulting in an isolator. Reversing the propagation direction is equivalent to reversing the direction of the applied field. Hence, we use the notation of $H(+)$ to represent propagation in the forward direction and $H(-)$ to represent propagation in the reverse direction. An isolator using Faraday rotation in a metal-ferromagnetic film requires a more complex structure and suffers from high loss [10].

A ferromagnetic–semiconductor composite (FSC) RL can consist of nanometer-size ferromagnetic particles distributed throughout a semiconductor host. The composites may be generated by epitaxial growth [11] or by ion implantation followed by annealing [12]. Such FSC layers can be used with semiconductor waveguides and integrated optic material systems. The optical loss of a composite consisting of nanometer-size-ferromagnetic particles in an FSC layer or in a plastic host material is reduced compared with a continuous ferromagnetic layer containing the same weight of ferromagnetic material, while the Faraday rotation and, hence, magnetooptic Kerr effects remains the same [13], [14]. For an FSC layer under bias by a magnetic field and with a thickness in the correct range to support the RLE, the relatively small change in complex refractive index between the positive and negative propagation direction causes the modal field of the waveguide to have a large secondary peak in the FSC layer in the reverse direction $H(-)$ and a much smaller one in the forward direction $H(+)$. This is illustrated in Fig. 7. For a given composition and choice of waveguide parameters, the required range of the FSC–RL thickness is determined by the waveguide conditions described in Section II.

An isolator example uses an FSC–RL of nanometer-size iron particles in an InGaAsP host within the InP p-cladding of a common 1.55-μm multi-quantum-well (MQW) laser structure as shown in Table II. This isolator can be integrated with a laser or amplifier. InGaAsP has a refractive index of 3.4, which is higher than the refractive index of the InP p-clad, which is 3.1628 at 1.55 μm. These values satisfy the need to have the real part of the refractive index of the FSC–RL greater than that of the p-clad. The cutoff thickness for the FSC–RL is shown in Table III. The volume fraction of Fe in the host is 0.020, and the reduction factor of the imaginary part of the complex refractive index is 1/30 [13].

The values of the complex refractive index and Faraday rotation of iron are obtained from Gaugitsch and Hauser [15], which gives recent values at a wavelength of 1.0 μm. These are adjusted to a wavelength of 1.55 μm using values given in [16]. We thus obtain a complex index for iron at a zero magnetic field of $n = 3.343$, $k = 5.104$. The Faraday rotation is $\Theta_F = 650\,000^\circ/\text{cm}$. The off-diagonal matrix element is given by $2n\Theta_F/k$. The Maxwell–Garnet theory [13] applied to a 2% volume fraction of nanometer-sized iron particles in an InGaAsP semconductor host of index 3.4 results in a complex index of the composite of $n = 3.4042$ and $k = 2.822 \times 10^{-3}$ (which corresponds to loss $\alpha = 228.8\ \text{cm}^{-1}$) for $H(+)$ and $n = 3.3930$ and $k = 4.146 \times 10^{-3}$ (which corresponds to a loss $\alpha = 336.2\ \text{cm}^{-1}$) for $H(-)$.

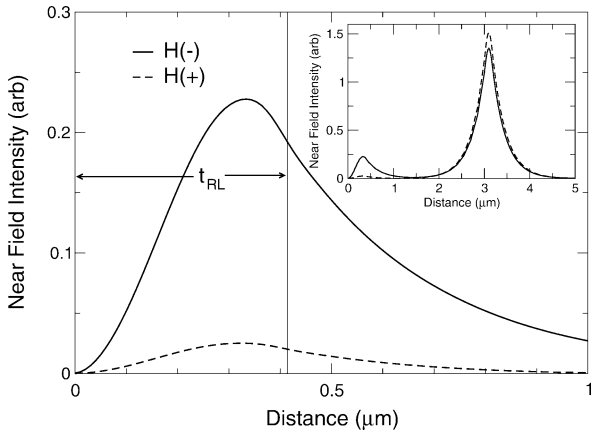

Fig. 7. Near-field intensity for an FSC RL showing the RLE on a multi-quantum-well (MQW) waveguide, $t_{\text{RL}} \approx 0.413\ \mu$m, and $t_C = 3.0\ \mu$m. Inset is the complete field intensity. The operating wavelength is $\lambda = 1.55\ \mu$m.

The isolator insertion loss and confinement factor for the FSC–RL at $\lambda = 1.55\ \mu$m as a function of the RL loss is shown Fig. 8. The RL thickness t_{RL} and clad thickness t_C are optimized values of 0.413 and 2.6 μm, respectively. The confinement factor maximum value is 0.247 at zero loss and drops to 0.238 at a loss value of $\approx$ 205 cm^{-1}, at which maximum isolation occurs.

The large difference in the amplitude of the secondary-field peak in the FSC–RL results in a large difference in the confinement factor (Γ_{RL}) for light traveling in opposite directions (Fig. 9). The large difference in Γ_{RL} effectively amplifies the effect of the loss of the RL. In addition, there is a change in the loss of the RL layer associated with the propagation direction due to the magnetooptic Kerr effect (shown in Table II), and the higher modal loss ($H(-)$ in Fig. 9) corresponds to the higher RL loss (336.2 cm^{-1} compared with 228.8 cm^{-1}). The resulting differences between $H(+)$ and $H(-)$ in the insertion loss of the waveguide mode yield high isolation and low insertion loss.

Fig. 10 shows the isolation and isolation–loss ratio as a function of the FSC–RL thickness. The isolation is the loss in the backward direction in decibels per centimeter. The isolation–loss ratio, which is the ratio of the loss in the backward direction to the loss in the forward direction in decibels per decibel, is also shown.

For an FSC–RL thickness of $t_{\text{RL}} \approx 0.413\ \mu$m, the isolation is 240 dB/cm with a forward insertion loss of only 12.7 dB/cm, giving an excellent isolation–loss ratio of 18.9 dB/dB. Thus, a 30-dB isolator could be 1.25 mm in length and have an insertion loss of 1.6 dB.

TABLE II
LAYER STRUCTURE FOR AN ISOLATOR USING FE–INGAASP FSC–RL DEPOSITED ON A TYPICAL MQW STRUCTURE USING QUATERNARY SEMICONDUCTOR LAYERS

Wavelength λ = 1.55 μm			
Layer Material	Loss, α (cm^{-1})	Refractive Index	Thickness (μm)
Air	0.0	1.0	-
Fe-InGaAsP FSC (H(+))	228.8	3.4042	See text
Fe-InGaAsP FSC (H(-))	336.2	3.3930	See text
p-clad InP	0.0	3.1628	3.0
Barrier InGaAsP	0.0	3.37	0.05
QW InGaAsP	0.0	3.46	0.01
Barrier InGaAsP	0.0	3.37	0.01
QW InGaAsP	0.0	3.46	0.01
Barrier InGaAsP	0.0	3.37	0.01
QW InGaAsP	0.0	3.46	0.01
Barrier InGaAsP	0.0	3.37	0.01
QW InGaAsP	0.0	3.46	0.01
Barrier InGaAsP	0.0	3.37	0.05
n-clad InP	0.0	3.1628	0.50
n-substrate InP	0.0	3.1628	-

TABLE III
FERROMAGNETIC–SEMICONDUCTOR COMPOSITE RL VALUES FOR OPERATION AT $\lambda = 1.55\ \mu$m

FSC Type	InGaAsP Host	p-clad		Cut off RL Thickness	Optimum RL Thickness	Max Isolation-Loss Ratio Is / L(+)
	n	n_C	t_C (μm)	h (μm)	t_{RL} (μm)	(dB/dB)
Fe-InGaAsP	3.4	3.163	2.6	0.22	0.413	22.9

V. MODULATORS USING THE RLE

An RL modulator on X-cut $LiNbO_3$ is illustrated in Fig. 11. A Ti–$LiNbO_3$-strip guide of width W_F is separated by $LiNbO_3$ strips of width W_C from two Ti–$LiNbO_3$ strips of width W_{RL}, which are doped to have loss. The doped lossy strips in this symmetric arrangement substitute for the RLs of the planar guides discussed previously. At the correct values of W_F, W_C, and W_{RL} and their corresponding effective indexes, secondary peaks of the guided intensity fall in the lossy strip regions. The secondary peaks "amplify" the effect of the loss strips. If the secondary peaks are large, the propagating mode has high losses (at resonance), and if the secondary peaks are small (off-resonance), the modal losses are small. The application of a voltage across the electrodes can change the refractive indexes of the strip guide, changing an on-resonance field distribution (with large secondary peaks) to an off-resonance distribution (with small or no secondary peaks), as illustrated by the near-field intensity plots of Fig. 12. The plots are made for a modulator with dimensions: $W_F = 3\ \mu$m, $W_C = 2\ \mu$m, and $W_{\mathrm{RL}} = 2.4\ \mu$m. The Ti diffusion depth is assumed to be 5 μm for both the guide and the lossy strips, and the optimum loss in the lossy strips is $\alpha_{\mathrm{RL}} = 233\ \mathrm{cm}^{-1}$.

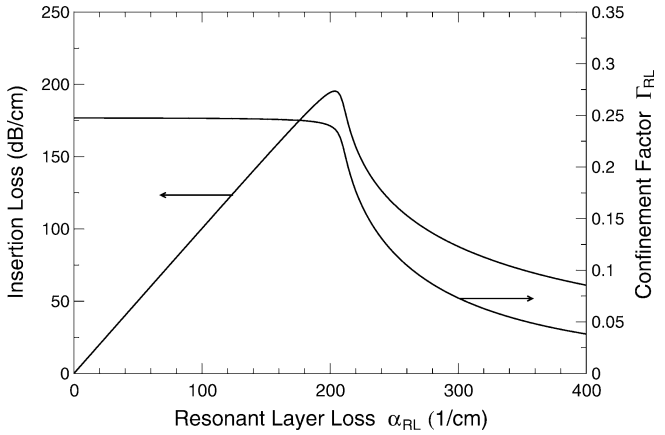

Fig. 8. For $H(-)$ biasing magnetic field, insertion loss and FSC–RL confinement factor at $\lambda = 1.55\ \mu$m as function of layer loss for ferromagnetic–semiconductor composite RL.

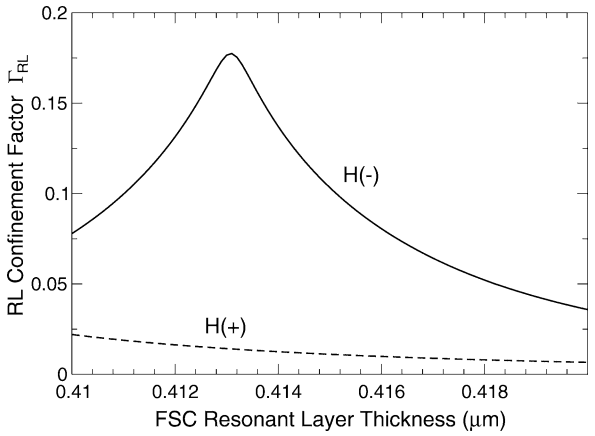

Fig. 9. Confinement factor of ferromagnetic–semiconductor composite RL showing RLE as the thickness of the FSC–RL is varied. Wavelength of operation is $\lambda = 1.55\ \mu$m.

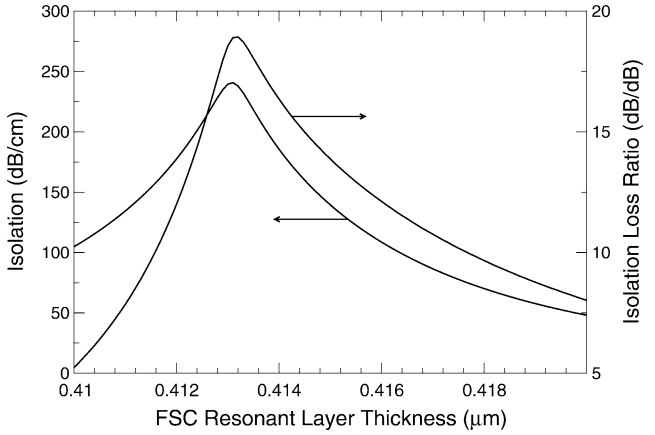

Fig. 10. Isolation and isolation–loss ratio as the thickness of the ferromagnetic–semiconductor composite (FSC) RL thickness is varied. Wavelength of operation is $\lambda = 1.55\ \mu$m.

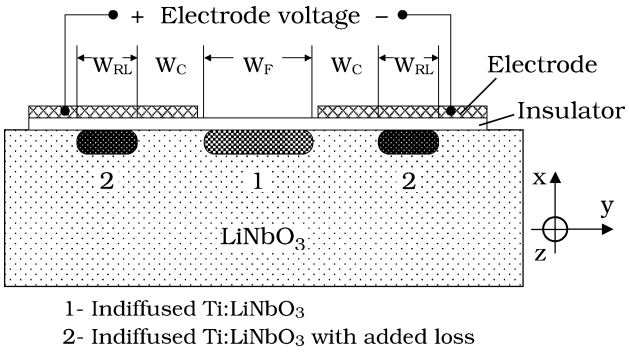

Fig. 11. $LiNbO_3$ RLE modulator using strip guides. Wavelength of operation is $\lambda = 1.523\ \mu$m.

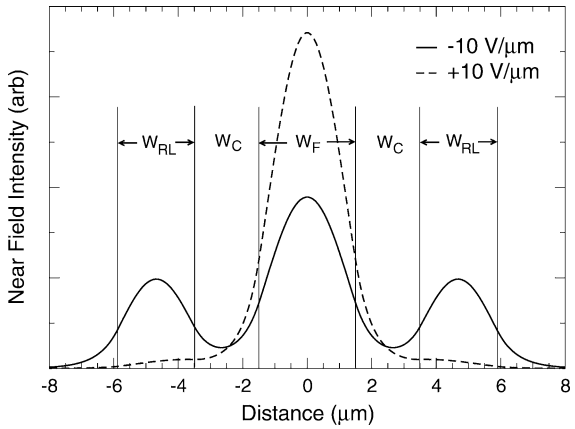

Fig. 12. $LiNbO_3$ RL modulator near-field plot. The voltage is applied across $W_F = 3\ \mu$m with $W_C = 2.0\ \mu$m and $W_{\rm RL} = 2.4\ \mu$m. Wavelength of operation is $\lambda = 1.523\ \mu$m.

At $V = -10\ \text{V}/\mu$m, the secondary peaks of the field intensity in the loss strip regions are large and at $V = 10\ \text{V}/\mu$m, there are no apparent secondary peaks. This example indicates the RLE in a device using strip guides with the effect in the lateral (y) direction rather than in the transverse (x) direction of the polarizer and isolators discussed previously.

The effective index method was used to calculate the field distributions of this device by solving for the lowest order planar TE modes of a 5-μm-thick layer of Ti–$LiNbO_3$ with and without loss on a $LiNbO_3$ substrate. The real and imaginary parts of the normalized propagation constant in both cases provide the effective refractive index and effective modal loss, respectively. The propagation constant of the TM mode of a planar guide with layers of thickness $W_{\rm RL}$, W_F, and W_C corresponding to the strips of Fig. 11 and using the appropriate effective values of refractive index and loss is then calculated to find the performance of the modulator. The refractive index [17] and loss values used are listed in Table IV for $\lambda = 1.523\ \mu$m. We assume that the material loss $\alpha_{\rm RL}$ does not change with applied voltage.

The insertion loss in decibels and the percent transmitted are plotted against voltage in Fig. 13 for a 300-μm-long device. The insertion loss ranges from 10.8 dB at $-10\ \text{V}/\mu$m to 0.87 dB at $+10\ \text{V}/\mu$m. The transmitted intensity varies from 18.2% to 82% over this range of voltage. For example, with $-3\ \text{V}/\mu$m dc bias, a $\pm$5-V/μm signal across W_F would give $\sim 45\%$ intensity modulation with an insertion loss of less than 7 dB in a device only 300 μm long. The short length minimizes the problem of phase matching between the driving signal and the optical wave. This length is short compared with lengths on the order of several centimeters, which is required by more conventional approaches to high-frequency optical modulators [17], [18].

VI. RLE-Enhanced Diffraction Gratings on Optical Waveguides

The sensitivity of the RLE to the thickness of the loss layer suggests fabricating diffraction gratings in such layers. As an example, consider the isolator waveguide structure described previously with layers shown in Table II and the isolation shown in Fig. 10. By forming a second-order outcoupling grating on the RL, the isolation loss can be substantially increased above 240 dB due to radiation with little or no increase in insertion loss.

Another possibility is the use of a low-loss (1–5 cm^{-1}) RL that produces a substantial secondary peak. In this case, a shallow grating on the RL at a modest distance from the core can provide very strong feedback or outcoupling compared with a typical grating formed in the cladding layer closer to the core.

TABLE IV
REFRACTIVE INDEX AND LOSS VALUES USED TO CALCULATE MODULATOR PERFORMANCE AT A WAVELENGTH OF 1.523 μm

	Ti-$LiNbO_3$		Effective		$LiNbO_3$
V/μm	Index	α_{RL} (cm^{-1})	Index	α_{EFF} (cm^{-1})	Index
-10	2.1563	-	2.1526	-	-
0	2.1583	233	2.1545	196	2.1383
10	2.1603	-	2.1565	-	-

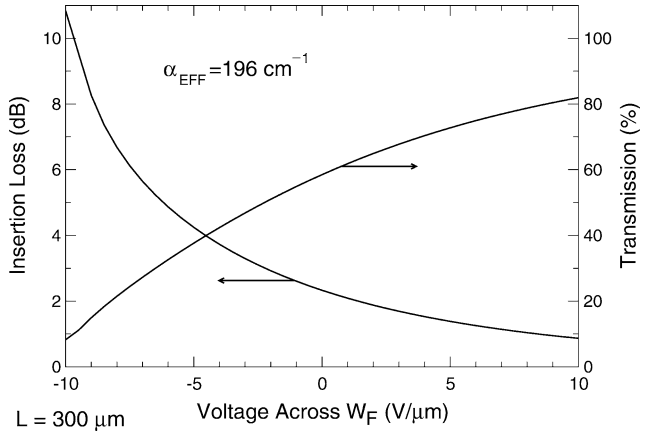

Fig. 13. $LiNbO_3$ RL modulator: $W_F = 3$ μm, $W_C = 2$ μm, $W_{RL} = 2.4$ μm, length = 300 μm, and $\alpha_{EFF} = 196$ cm^{-1}. Wavelength of operation is $\lambda = 1.523$ μm.

VII. CONCLUSION

A high-refractive-index layer containing a prescribed thickness and amount of loss added to the cladding layer of an optical waveguide can act to enhance the operation of waveguide polarizers, isolators, modulators, and diffraction gratings. The waveguide loss becomes very sensitive to small changes in waveguide properties because of the appearance of a secondary-field peak in the added RL at the prescribed thickness. This effect is called the RLE. The RLE enhances the isolation and reduces the insertion loss of isolators, increases the polarization ratio and reduces the insertion loss of polarizers, reduces the length of electrooptic modulators, and increases the feedback and outcoupling of diffraction gratings. Polarizers, isolators, filters, and electrooptic-intensity modulators that can be integrated with a variety of material systems and showing excellent properties using the RLE have been described.

Possible dimensions and compositions required to illustrate devices based on the RLE are provided. Although reasonable performance parameters are calculated, no attempt was made to fully optimize these devices.

APPENDIX

In a gyrotropic medium exhibiting the magnetooptic Kerr effect, the relative dielectric tensor can be written as a tensor whose components depend on the direction of an applied magnetic field. In particular, when the static magnetic field is applied in the y direction of a dielectric layer containing the spin-oriented material, the dielectric tensor becomes

$$\overleftrightarrow{\kappa} = \kappa_g \begin{pmatrix} 1 & 0 & jQ \\ 0 & 1 & 0 \\ -jQ & 0 & 1 \end{pmatrix} \tag{A1}$$

where κ_g and Q are complex quantities associated with the anisotropic layer. In other layers, say the ith layer, which is assumed to be isotropic, the off-diagonal element $jQ = 0$ and the relative dielectric constant is κ_i.

It is now appropriate to discuss waves in a multilayered dielectric waveguide with mode propagation in the positive z direction. The relative permittivity will be assumed to be constant in each layer of the structure. For "TE"- polarized fields, the electric field has only a component in the y direction E_y, while the magnetic field has two components H_x and H_z. The Maxwell equation that includes the gyrotropic properties is

$$\nabla \times \mathbf{H} = j\omega\varepsilon_0 \overleftrightarrow{\kappa} \cdot \mathbf{E}. \tag{A2}$$

For an electric field polarized along y, the right-hand side (RHS) of (A2) is identical to that for a nongyrotropic medium because the product of the dielectric tensor and electric field has only a component in the y direction. (The gyrotropic variable Q plays no role in the solution of Maxwell's equation.) Accordingly, the waves behave similar to those in an isotropic material.

The gyrotropic medium affects the "TM"-polarized waves considerably different than the "TE"-polarized waves. For "TM"- polarized modes, there is only one component of the magnetic field H_y, while the electric field has both E_x and E_z. Here, the RHS of (A2) couples the E_x and E_z components so that

$$\overleftrightarrow{\kappa} \cdot \mathbf{E} = \hat{\mathbf{x}}\kappa_g(E_x + jQE_z) + \hat{\mathbf{z}}\kappa_g(-jQE_x + E_z) \tag{A3}$$

where $\hat{\mathbf{x}}$ and $\hat{\mathbf{z}}$ are unit vectors in the x and z directions, respectively. The wave equation for H_y, found from the two Maxwell curl equations, is

$$\frac{d^2H_y}{dx^2} + h_g^2 H_y = 0 \tag{A4}$$

where the transverse wavenumber of the gyrotropic medium is

$$h_g^2 = (\gamma^2 + k^2\kappa_g)(1 - Q^2). \tag{A5}$$

The magnetic field H_y and the electric field component E_z must be continuous at the boundary between the gyrotropic material and the surrounding layers. Continuity of the electric field

E_z is assured if the following expression, which we label as "flux," is continuous

$$j\omega\varepsilon_0 E_z = \frac{1}{\kappa_g(1-Q^2)}\left(jQ\gamma H_y + \frac{dH_y}{dx}\right). \tag{A6}$$

For most practical structures where layers have modest fractional content of gyrotropic materials such as Fe or Co, the value of $Q \ll 1$ so that the transverse wavenumber given by (A5) has the form

$$h_g^2 = \gamma^2 + k^2\kappa_g \tag{A7}$$

which has the same form as that of an isotropic layer. Hence, the anisotropic behavior of the mode is determined entirely from the flux continuity, (A6), which is now reduced to (first order in Q)

$$j\omega\varepsilon_0 E_z \approx \frac{1}{\kappa_g}\left(jQ\gamma H_y + \frac{dH_y}{dx}\right). \tag{A8}$$

ACKNOWLEDGMENT

The authors would like to thank T. Masood and S. Patterson, both of Photodigm, Inc., Richardson, TX, for technical discussions.

REFERENCES

[1] G. A. Evans, B. Goldstein, and J. K. Butler, "Observations and consequences of nonuniform aluminum concentrations in the channel regions of AlGaAs channeled-substrate-planar lasers," *IEEE J. Quantum Electron.*, vol. QE-23, pp. 1900–1908, Nov. 1987.

[2] J. M. Hammer, "Modulation and switching of light in dielectric waveguides," in *Integrated Optics*, T. Tamir, Ed. New York: Springer-Verlag, 1975, ch. 4, pp. 185–189.

[3] J. K. Butler, N. H. Sun, G. A. Evans, L. Pang, and P. Congdon, "Grating-assisted coupling of light between semiconductor and glass waveguides," *J. Lightwave Technol.*, vol. 16, pp. 1038–1048, June 1998.

[4] H. Kogelnik, "Theory of dielectric waveguides," in *Integrated Optics*, 2nd ed, T. Tamir, Ed. New York: Springer-Verlag, 1982, pp. 24–25.

[5] R. Smith and G. Mitchell, "Calculation of complex propagating models in arbitrary, plane layered, complex dielectric structures," Univ. of Washington, Seattle, EE Tech. Rep. 206 , 1977.

[6] J. Ballato, S. Foulger, and D. W. Smith, Jr., "Optical properties of perfluorocyclobutyl polymers," *J. Opt. Soc. Amer. B, Opt. Phys.*, vol. 20, pp. 1838–1843, Sept. 2003.

[7] W. Zaets and K. Ando, "Optical waveguide isolator based on nonreciprocal loss/gain of amplifier covered by ferromagnetic layer," *IEEE Photon. Technol. Lett.*, vol. 11, pp. 1012–1014, Aug. 1999.

[8] Y. Okamura, T. Negate, and S. Yamamoto, "Integrated optical isolator and circulator using nonreciprocal phase shifters: A proposal," *Appl. Opt.*, vol. 23, pp. 1866–1889, June 1984.

[9] T. Mizumoto, K. Oochi, T. Harada, and Y. Naito, "Measurement of optical nonreciprocal phase shift in Bi-substituted GdFeO film and application to waveguide type optical circulators," *J. Lightwave Technol.*, vol. 4, pp. 347–352, Mar. 1986.

[10] J. M. Hammer, J. H. Abeles, and D. J. Channin, "Polycrystalline-metal-ferromagnetic optical waveguide isolator (POWI) for monolithic-integration with diode-laser devices," *IEEE Photon. Technol. Lett.*, vol. 9, pp. 631–633, May 1997.

[11] H. Shimizu and M. Tanaka, "Design of semiconductor-waveguide-type optical isolators using the nonreciprocal loss/gain in the magneto-optical waveguides having MnAs nanoclusters," *Appl. Phys. Lett.*, vol. 81, no. 27, pp. 5246–5248, Dec. 2002.

[12] J. D. Budai, C. W. White, S. P. Withrow, M. F. Chisholm, J. Zhu, and R. A. Zuhr, "Controlling the size, structure and orientation of semiconductor nanocrystals using metastable phase recrystallization," *Nature*, vol. 390, pp. 384–386, Nov. 1997.

[13] K. Baba, F. Takase, and M. Miyagi, "Ferromagnetic particle composite polymer films for glass and semiconductor substrates," *Opt. Commun.*, vol. 139, pp. 35–38, June 1997.

[14] ——, "Magnet-optic media composed of ferromagnetic metal island films for glass and semiconductor substrates," *Electron. Lett.*, vol. 32, no. 16, pp. 222–223, Feb. 1996.

[15] M. Gaugitsch and H. Hauser, "Optimization of a magneto-optical light modulator—Part II: Modeling and measurement of Faraday and Kerr effects," *J. Lightwave Technol.*, vol. 17, pp. 2645–2657, Dec. 1999.

[16] R. C. Weast, Ed., *CRC Handbook of Chemistry and Physics*, 67th ed. Boca Raton, FL: CRC, 1986–1987, p. E-382.

[17] J. Kondo, A. Kondo, K. Aoki, M. Imaeda, T. Mori, Y. Mizuno, S. Takatsuji, Y. Kozuka, O. Mitomi, and M. Minikata, "40-Gb/s X-cut $LiNbO_3$ optical modulator with two-step back-slot structure," *J. Lightwave Technol.*, vol. 20, pp. 2110–2113, Dec. 2002.

[18] A. Long, J. Buck, and R. Powel, "Design of an opto-electronic modulator driver amplifier for 40-Gb/s data rate system," *J. Lightwave Technol.*, vol. 20, pp. 2015–2021, Dec. 2002.

Jacob M. Hammer (SM'62–F'88–LF'96) received the B.S. degree in engineering physics from New York University, New York, in 1950, the M.S. degree in physics from the University of Illinois at Urbana-Champaign in 1951, and the Ph.D. degree in physics from New York University in 1956.

He was a Member of the Technical Staff at Bell Telephone Laboratories from 1956 to 1959. He then joined the technical staff of RCA Laboratories (now Sarnoff Corporation), where he developed the lowest noise figure (1-dB) microwave traveling-wave tube ever reported. In 1968, he was a Senior Visitor at the Cavendish Laboratory, Cambridge University, Cambridge, U.K. In 1969, he returned to RCA, where he made important contributions to single-crystal optical waveguides and modulators, coauthoring the first report of metal-indiffused lithium tantalate, lithium niobate optical waveguides and modulators. In 1987, he left RCA Laboratories to found Photonics Consulting, Annapolis, MD, where he currently works on optical waveguide devices. He has 28 patented inventions, more than 100 publications, is co-editor of the book *Surface Emitting Semiconductor Lasers* (New York: Academic, 1993), and has contributed chapters about modulators to two books on integrated optics.

Dr. Hammer is a Member of the American Physical Society (APS) and the Optical Society of America (OSA). He was Associate Editor of the IEEE JOURNAL OF QUANTUM ELECTRONICS from 1987 to 1989. He served on the Optical Communications Task Force of the U.S. Department of Commerce from 1975 to 1981.

Gary A. Evans (S'69–M'75–SM'82–F'92) was born in Omak, WA. He received the B.S.E.E. degree from the University of Washington, Seattle, in 1970 and the M.S. degree in electrical engineering and the Ph.D. degree in electrical engineering and physics from the California Institute of Technology (Caltech), Pasadena, in 1971 and 1975, respectively.

After a postdoctoral year at Caltech, he worked for R&D Associates, Marina Del Rey, CA, and was a Visiting Assistant Professor in the Electrical Engineering Department at the University of Washington (1977–1979). He has worked at the Aerospace Corporation, El Segundo, CA (1979–1981), TRW, Redondo Beach, CA (1981–1984), and RCA Laboratories (now Sarnoff Corporation), Princeton, NJ (1984–1992). In 1992, he joined the Electrical Engineering Department, Southern Methodist University, Dallas, TX, as a Professor. He is a Founder and Member of the Board of Directors of Photodigm, Inc., Richardson, TX. Since 1979, he has primarily worked on the design, growth, and fabrication of conventional cleaved facet and grating surface-emitting semiconductor lasers. He has more than 220 publications, ten patents, and is a co-editor of the book *Surface Emitting Semiconductor Lasers* (New York: Academic, 1993).

Dr. Evans is a Member of the Optical Society of America (OSA). He was elected a Fellow of the IEEE for "contributions to the development, fabrication, and understanding of semiconductor lasers." He was formerly an Associate Editor of the IEEE JOURNAL OF QUANTUM ELECTRONICS (1989–1995). He has served on numerous IEEE committees and is a past Chairman of the Princeton, NJ, and Dallas, TX, Sections of the Lasers and Electro-Optics Society (LEOS), a past Chairman of the Santa Monica Bay Section of the IEEE, a former Finance Chairman for the 1994 IEEE International Semiconductor Laser Conference, and a former Technical Program Vice Chair for the 1996 International Communications Conference. He is a licensed Professional Engineer.

Gokhan Ozgur (S'01) was born in Isparta, Turkey, in 1971. He received the B.S. degree in electrical and electronics engineering from the Middle East Technical University, Ankara, Turkey, in 1993 and the M.S. degree in electronics engineering from Fatih University, Istanbul, Turkey, in 2001. He is currently working toward the Ph.D. degree with the Electrical Engineering Department, Southern Methodist University, Dallas, TX.

He worked as an Instructor and Network Administrator in the Computer Engineering Department at Ataturk Alatoo University, Bishkek, Kyrgyzstan (1997–1999) and as a Graduate Research Assistant in the Electronics Engineering Department at Fatih University (1999–2001). He is currently a Graduate Research Assistant in the Electrical Engineering Department at Southern Methodist University, working on the design, fabrication, and testing of optical isolators integrated with semiconductor lasers. His research interests include long-wavelength semiconductor lasers, electrooptical and magnetooptical effects in optoelectronic devices, wavelength-division-multiplexing (WDM) fiber-optic communication systems, and microelectromechanical system (MEMS) devices.

Jerome K. Butler (S'59–M'65–SM'78–F'89) was born in Shreveport, LA. He received the B.S.E.E. degree from Louisiana Polytechnic Institute, Ruston, in 1960 and the M.S.E.E. and Ph.D. degrees from the University of Kansas, Lawrence, in 1962 and 1965, respectively.

He was a Research Assistant and held a CRES Fellowship at the Center for Research in Engineering Sciences, University of Kansas. He conducted research concerned with electromagnetic-wave propagation and the optimization and synthesis techniques of antenna arrays. In the summers from 1969 to 1990, he was a Staff Scientist at the David Sarnoff Research Center RCA Laboratories, Princeton, NJ. From 1996 to 1997, he was on sabbatical leave with the Photonics and Micromachining System Components Laboratory at Texas Instruments. He has held consulting appointments with Photodigm, Inc., Richardson, TX; the Photonics and Micromachining System Components Laboratory at Texas Instruments; the Central Research Laboratory of Texas Instruments; the Geotechnical Corporation of Teledyne, Inc.; Earl Cullum Associates of Dallas, TX; and the University of California Los Alamos Scientific Laboratory, Los Alamos, NM. He is coauthor of the book *Semiconductor Lasers and Heterojunction LED's* (New York: Academic, 1977). He joined the faculty of the School of Engineering and Applied Science, Southern Methodist University, Dallas, TX, where he is now a University Distinguished Professor of Electrical Engineering. His current primary research areas are solid-state injection lasers, radiation and detection studies of lasers, millimeter-wave systems, integrated optics and the application of integrated optical circuits, and quantum electronics.

Dr. Butler received the Southern Methodist University Sigma Xi Research Award in 1977 and was elected a Fellow of the IEEE for his contributions to semiconductor lasers and the radiation characteristics of optical waveguides. He is a Member of Sigma Xi, Tau Beta Pi, and Eta Kappa Nu. He is a registered Professional Engineer in the State of Texas.